CHAPTER 7
APPLICATION OF VOUSSOIR BEAM AND PLATE BUCKLING THEORY

7.1 INTRODUCTION

Independent checks on aspects of the numerical models that were introduced in Chapter 5 and Chapter 6 are the subject of consideration in this chapter. Voussoir beam theory will be applied to the models developed in Chapter 5 to corroborate the ability of the models in simulating the deflection of the Bulgo Sandstone, and plate buckling theory will be applied to the models developed in Chapter 6 to corroborate the ability of the models in predicting valley base yield.

7.2 APPLICATION OF VOUSSOIR BEAM THEORY

A basic derivation and how to use voussoir beam theory from Sofianos (1996), Sofianos and Kapenis (1998) and Nomikos, Sofianos and Tsoutrelis (2002) can be found in Appendix E. This theory has been used to calculate the theoretical deflection of the Bulgo Sandstone in Models 1 to 4.

The results from Models 1 to 4 (Chapter 5) indicated that the Bulgo Sandstone was the massive spanning unit in the overburden and the majority of the caving was confined below the base of the massive unit. This was the case for Model 2, whilst failure extended into the Bulgo Sandstone in Models 3 and 4. It was noted that caving was not sufficient enough to produce any measurable goaf angle in Model 1, therefore this model could not be analysed with the voussoir beam method. The geometry of the cave zone was defined by a goaf angle of 11° to 25° for Model 2, 14° to 25° for Model 3 and 13° to 25° for Model 4.

In order to perform an analysis, the following parameters must be known:

- Longwall panel width (m),
- Cover depth (m),
- Hawkesbury Sandstone thickness (m),
- Newport Formation thickness (m),
- Bald Hill Claystone thickness (m),
- Bald Hill Claystone density (kg/m^3),
- Bulgo Sandstone thickness (m),
- Bulgo Sandstone density (kg/m^3),
- Bulgo Sandstone Young's Modulus (MPa),
- Cave zone height (m), and
- Goaf angle (°).

See Figure 2.1 for a definition on caving height and goaf angle.

It is important to note that the analysis is actually performed on the base of the Bulgo Sandstone as defined by the bedding plane spacing and extent of failure into the spanning unit, and using the notion that thinner bedded layers load thicker bedded layers (Obert & Duvall 1967), it is only the Bald Hill Claystone that acts as a surcharge on the Bulgo Sandstone (see Table 5.5).

For example, if the Bulgo Sandstone is 92 m thick with a bedding plane spacing of 9 m, the Bald Hill Claystone 12 m thick and the cave zone penetrates 64 m into the Bulgo Sandstone, the analysis would be performed on the bottom 9 m of unbroken Bulgo Sandstone with that layer being loaded by a surcharge of 31 m. The area and weight of the surcharge was defined by the goaf angle and the weighted average density of the surcharge. Using the procedure described in Appendix E, a simple spreadsheet was set up to calculate the deflection of the Bulgo Sandstone for each model geometry. It was found that the calculated deflections were highly sensitive to the goaf angle value. However, there was agreement within the confines of the simple model for the goaf angle. Table 7.1 contains the analytical and numerical deflection of the Bulgo Sandstone.

Table 7.1 – Analytical and numerical deflection of the Bulgo Sandstone

Model	UDEC Deflection (mm)	UDEC Goaf Angle (°)	Back-Calculated Goaf Angle (°)
2	275	11 – 25	20.0
3	345	14 – 25	11.6
4	506	13 – 25	12.5

7.3 APPLICATION OF PLATE BUCKLING THEORY

The UDEC models in Chapter 6 produced behaviour that may indicate the onset of yield in the base of the valleys of the type shown in Chapter 3. For the models that contained the translation plane below the base of the valley, with no joints in the beam formed by the translation plane, the maximum average horizontal stress immediately below the sides of the valleys ranged from 18 MPa to 65 MPa.

Hoek and Brown (1980) provided a comprehensive overview of plate buckling theory, and stated that the axial stress at which a plate will buckle is given by (Equation 7.1):

$$\sigma_\alpha = \frac{\pi^2 E}{12q^2(l/t)^2} \qquad [7.1]$$

Where,

σ_α = Axial stress required for buckling (MPa)
E = Elastic or Young's Modulus (MPa)
q = A constant (0.5 for both ends clamped)
l = Length of plate (m)
t = Thickness of plate (m)

Equation 7.1 can be rearranged so that the critical thickness of a plate can be determined if the axial stress is already known (Equation 7.2):

$$t = \frac{l}{\sqrt{\pi^2 E/\sigma_\alpha(12q^2)}} \qquad [7.2]$$

Figure 7.1 illustrates the critical thickness for beams given an average horizontal stress for different valley widths.

It can be seen from Figure 7.1 that when the values of maximum average horizontal stresses in the river valley models (18 MPa – 65 MPa) are applied to this graph, the calculated thickness of the beam that would buckle for a 50 m wide valley is in the order of 1 m to 1.9 m. This is corroborated by the author's recollection of buckling in a similar geographical location where buckled slabs were usually 0.5 m to 1 m thick, and rarely exceeded 2 m in thickness. Simple buckling (Figure 7.2) and low angle shear (Figure 3.6) were common features in the field.

7.4 SUMMARY

Two analytical solutions were introduced and applied to the river valley numerical models in an attempt to further test the credibility of the numerical models. This was undertaken to provide a possible means of analysing a complex problem with simple analytical tools and to assess whether there was any merit in using any of the solutions in the future. It was seen that the numerical models complied with both analytical solutions. Voussoir beam theory back-calculated goaf angles that were in general agreement with the goaf angles produced by UDEC, and the plate buckling solution (along with the author's recollection of buckling events) suggested that the horizontal stresses produced by the UDEC modelling is in the vicinity of what is required to buckle the valley floor for the valley geometry modelled. The critical thickness of the slabs calculated by the plate buckling analogue corresponds to field observations.

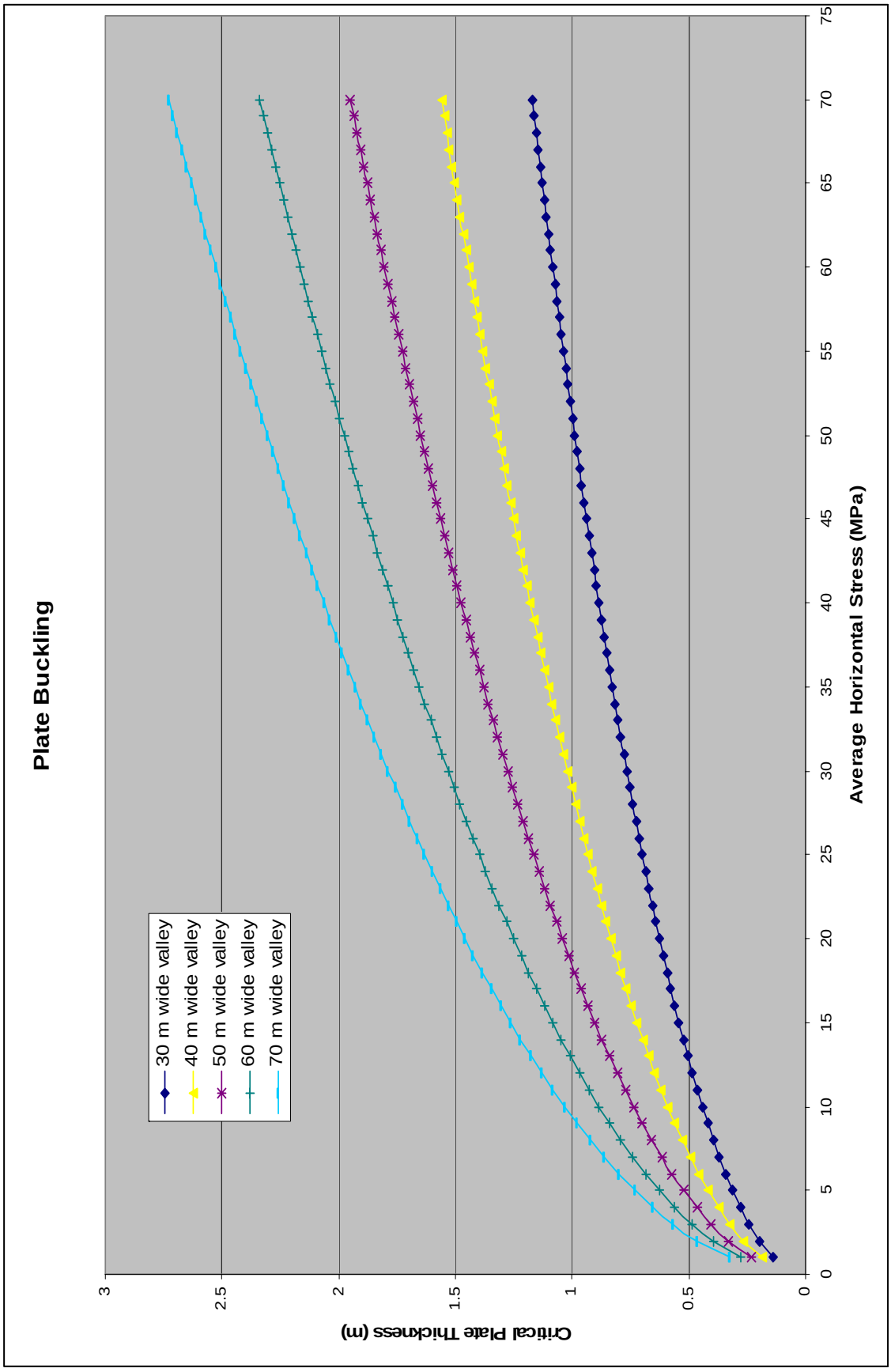

Fig. 7.1 – Critical plate thickness for buckling

Fig. 7.2 – Simple buckling in the field